2011 American Control Conference
on O'Farrell Street, San Francisco, CA, USA
June 29 - July 01, 2011

# Dynamic Gain-Scheduling Controller Design for Port-Fuel-Injection Processes

Andrew White, Jongeun Choi, and Guoming Zhu

*Abstract*— **In this paper, an event-based dynamic gain-scheduling controller was designed by employing a standard control structure of observer-based state feedback with integral control. The dynamic gain-scheduling controller was applied to an LPV system representing the air-to-fuel ratio control of a port-fuel-injection process. The system parameters used in the engine fuel system model are engine speed, temperature, and load. The static gains of the dynamic gain-scheduling controller for the obtained LPV system were then designed based on the numerically efficient convex optimization (or LMI) technique. The simulation results demonstrate the effectiveness of the proposed scheme.**

## I. Introduction

Increasing concerns about global climate change and ever-increasing demands on fossil fuel capacity call for reduced emissions and improved fuel economy of internal combustion (IC) engines. The control of air-to-fuel ratio in vehicles with a three-way catalyst is an extremely important control problem. Spark-ignited internal combustion engines are operated at a desired air-to-fuel ratio since the highest conversion efficiency of a three-way catalyst occurs around stoichiometric air-to-fuel ratio.

There have been several fuel control strategies developed for internal combustion engines to improve the efficiency and exhaust emissions. A key development in the evolution was the introduction of a closed-loop fuel injection control algorithm [1], followed by the linear quadratic control method [2], and an optimal control and Kalman filtering design [3]. Specific applications of A/F ratio control based on observer measurements in the intake manifold were developed by [4]. Another approach was based on measurements of exhaust gases A/F ratio measured by the oxygen sensor and the mass air flow rate close to the throttle position [5]. Ref. [6] also developed a nonlinear sliding mode control of A/F ratio based upon the oxygen sensor feedback. Continuing research efforts of A/F ratio control include adaptive approaches [7], [8], observer-based controllers [9], $H_\infty$ controllers [10], model predictive controllers [11], sliding mode controllers [12], and linear parameter-varying controllers [13], [14], [15], [16], [17]. Conventional A/F ratio control for automobiles uses both closed-loop feedback and feedforward control to have good steady state and fast transient responses.

For a spark-ignited engine equipped with a port-fuel-injection system, the wall-wetting dynamics is commonly used to model the fuel injection process; and the wall-wetting effects are compensated on the basis of simple time-invariant linear models that are tuned and calibrated through engine dynamometer and vehicle tests. These models are quite effective for an engine operated at steady state or slow transition conditions but they are difficult to be used at fast transient and other special operational conditions, for instance, during engine cold start. One of the approaches to model the wall-wetting dynamics during engine cold start is to describe it using a family of linear models to approximate the system dynamics at different engine cylinder head temperature, speed and load conditions, that is, to translate the fuel system model into a linear parameter varying (LPV) system.

As stated earlier, the use of LPV modeling to control the A/F ratio of a port-fuel-injection system has been reported by [13], [14], [15], [16] and [17]. In [15], a continuous-time, LPV model is developed considering only engine speed as a time-varying parameter. Due to the simplicity of the model used, the issue of engine cold start is not addressed. Furthermore, the control synthesis method used in [15] relies on gridding the parameter space at a finite number of grid points. In [14], a large variable time delay is present in the air-fuel ratio control loop for a lean burn spark ignition engine. LPV control methods are used to compensate for the variable time delay. In [13], a discrete-time, LPV model is developed with manifold absolute pressure, exhaust valve closing, and inlet valve opening as the time-varying parameters. However, only manifold absolute pressure is used as a scheduling parameter in the gain-scheduling control that is synthesized. Also, [13] does not address the issue of engine cold start. Additionally, all LPV control synthesis methods used by [13] are based in continuous time, relying on Tustin's (bilinear) transformation to convert the discrete-time system to a continuous-time system, thus fixing the engine speed and sampling rate of the discrete-time system. In [16] and [17], event-based gain-scheduling proportional-integral (PI) and proportional-integral-derivative (PID) controllers are developed. The control structure and design process for the event-based gain-scheduling PI controller is covered in [16]. The addition of derivative control to obtain gain-scheduling PID controllers is covered in [17]. Although the gain-scheduling PI and PID controllers designed and simulated in [16] and [17] show good steady-state and transient response, we believe that the performance can be further improved using a dynamic controller.

The purpose of this paper is to develop an event-based, dynamic gain-scheduling controller for an event-based, discrete-time LPV system with wall-wetting parameters and engine speed as time-varying parameters. To design

Andrew White, Jongeun Choi and Guoming Zhu are with the Department of Mechanical Engineering, Michigan State University {whitea23, jchoi, zhug}@egr.msu.edu

978-1-4577-0079-8/11/$26.00 ©2011 AACC

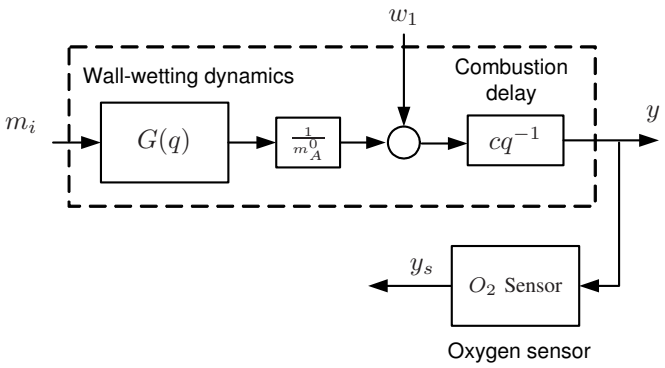


Fig. 1. The block diagram of the port-fuel-injection process and sensor dynamics.

the dynamic gain-scheduling controller, a standard control structure of observer-based state feedback with integral control was employed. To cope with practical situations, the discrete-time LPV control synthesis method given by [18] is used to develop the event-based, gain-scheduling state-feedback, integral, and observer gains. An affine LPV model including the dynamics of the system, the feedforward controller, and the observer is obtained. Gain-scheduling controllers have been synthesized to guarantee the robust stability and performance of the affine LPV model.

The paper is organized as follows. The dynamics of the port-fuel-injection process and oxygen sensor are reviewed in Section II. In Section III the LPV gain-scheduling controller design method is provided. Simulation results of the dynamic gain-scheduling controller are provided in Section IV. Concluding remarks are in the final section.

Standard notation is used throughout the paper. Let $\mathbb{R}$ and $\mathbb{Z}_{\geq 0}$ denote the set of real and non-negative integer numbers. The positive definiteness of a matrix $A$ is denoted by $A \succ 0$. The maximum (respectively, minimum) of $\alpha$ is denoted by $\overline{\alpha}$ (respectively, $\underline{\alpha}$). The abbreviation LFT is used to denote a linear fractional transformation. Furthermore, an upper LFT is denoted by $\mathcal{F}_u$. An identity matrix of size $n$ is denoted by $I_n$. Other notation will be explained in due course.

## II. Plant dynamics

In this section, the dynamics of the plant (Fig. 1), which are covered in full detail by [16], will be briefly reviewed.

### A. Dynamics of the port-fuel-injection process

The discrete-time linear system is obtained by event-based sampling of the port-fuel-injection process; hence the sampling time of this discrete-time system is the period of an engine cycle,

$$t_s = \frac{1}{v}\frac{\text{min.}}{\text{rev.}}\left(\frac{60\text{ sec.}}{1\text{ min.}}\right)\left(\frac{2\text{ rev.}}{1\text{ cycle}}\right) = \frac{120}{v}\frac{\text{sec.}}{\text{cycle}}, \quad (1)$$

where $v$ represents the engine speed in revolutions per minute (rpm) (see general engine modeling techniques in [19]).

The wall-wetting dynamics can be described as follows:

$$\begin{aligned} m_w(k) &= (1-\beta_k)m_i(k) + (1-\alpha_k)m_w(k-1), \\ m_c(k) &= \beta_k m_i(k) + \alpha_k m_w(k-1), \end{aligned} \quad (2)$$

where $k \in \mathbb{Z}_{\geq 0}$, and $m_i$, $m_w$, and $m_c$ denote the amount of fuel, injected, on the wall, and in the cylinder respectively. The coefficients $\alpha \in [0,\ 1]$, and $\beta \in [0,\ 1]$, are the ratios of the fuel delivered from the wall to the cylinder, and of the fuel entering the cylinder from injection, respectively. These values can be estimated online through an available set of engine sensors, which allows us to apply gain-scheduling control to the plant. Using the discrete-time dynamics in Eq. (2), we obtain the transfer function $G(q)$ from $m_i$ to $m_c$

$$G(q) := \frac{m_c(k)}{m_i(k)} = \frac{\beta_k + (\alpha_k - \beta_k)q^{-1}}{1-(1-\alpha_k)q^{-1}}, \quad (3)$$

where $q$ is the *forward shift operator* that satisfies

$$qu(k) = u(k+1).$$

The dotted box in the block diagram in Fig. 1 illustrates the fuel-injection process. The output of $G(q)$ is the input to the gain block of $\frac{1}{m_A^0}$, which is the nominal value of the inverse of the air amount $m_A$. The signal $w_1$ represents the deviation $\left(\frac{m_c}{m_A} - \frac{m_c}{m_A^0}\right)$, which will be treated as a disturbance in this paper. Another constant gain factor $c = 14.6$ in Fig. 1 is the value for the air-to-fuel-ratio at stoichiometric. After the combustion delay block the equivalence ratio $y$ is generated.

### B. Oxygen sensor

To measure $y$, we use an oxygen sensor placed downstream from the exhaust valve. The transport delay of the exhaust gas mixture is modeled as a function of engine speed, $T_D = \frac{80}{v}$, where $v$ denotes the engine speed in revolutions per minute (rpm). The combined transfer function in the continuous time domain is

$$y_s(s) = \frac{\exp(-T_D s)}{T_{O_2}s + 1}y(s), \quad (4)$$

where $y_s$ is the equivalence ratio measured by the sensor and $T_{O_2}$ is the time constant of the oxygen sensor. The details regarding the discretization and parameterization of Eq. (4) are covered in [16].

### C. An LPV system

The state-space representation of the port-fuel-injection dynamics combined with the oxygen sensor dynamics is given by

$$\begin{aligned} x_p(k+1) &= A_p(\Theta)x_p(k) + B_w w_1(k) + B_p(\Theta)m_i(k) \\ y_s(k) &= C_p x_p(k) \end{aligned} \quad (5)$$

where $x_p(k) \in \mathbb{R}^s$ is the state of the plant at time $k$ and $\Theta$ is the compact notation used to denote the time varying wall-wetting parameters and engine speed. The specific structure of $\Theta$ is given in the next section.

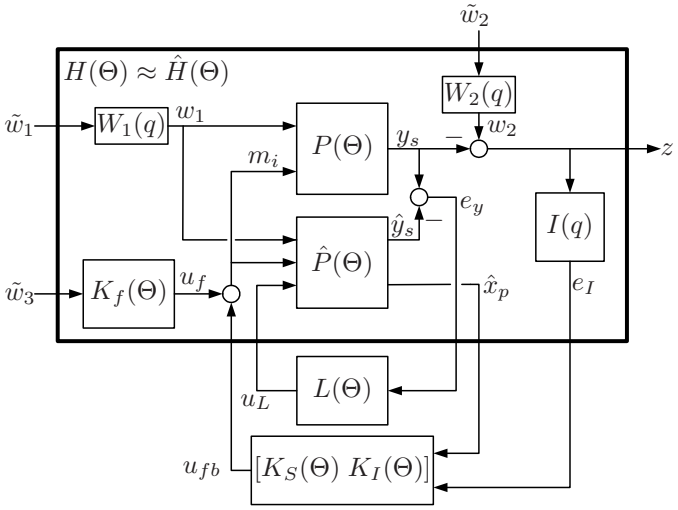


Fig. 2. The proposed control strategy for the fuel injection process (without the weighting functions $W_1(q)$ and $W_2(q)$, which are used only for controller synthesis). The LPV controller synthesis is applied to the first-order Taylor series expansion of the systems inside of the box to obtain the controller gains $K_S(\Theta)$, $K_I(\Theta)$, and $L(\Theta)$.

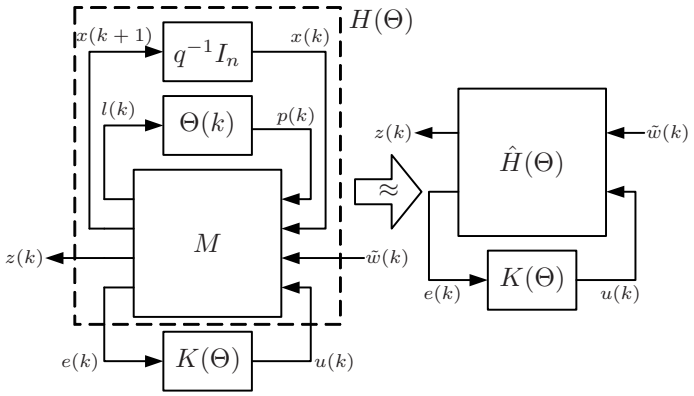


Fig. 3. The discrete-time LPV system $H(\Theta)$ with LFT parameter dependency displayed in the standard LFT configuration as shown in Eq. (8). The first-order Taylor series expansion of $H(\Theta)$ is computed to obtain $\hat{H}(\Theta)$, which has affine functions in $\Theta$. The LPV controller synthesis is applied to the affine LPV system $\hat{H}(\Theta)$ to obtain the controller $K(\Theta)$ in Eq. (7).

## III. LPV GAIN-SCHEDULING CONTROLLER DESIGN

### A. Control Strategy

The objective of the control system is to regulate the equivalence ratio $y$ to a reference input $w_2$ using feed-forward and feedback control against the disturbance signal $w_1$ and the time-varying wall-wetting dynamics and engine speed. In particular, we want to guarantee the stability of the closed-loop system and also minimize the effect of the disturbances for any combination of the wall-wetting dynamics and engine speed variations. The proposed control strategy is illustrated in Fig. 2. This scheme has six components, that is a feed-forward controller $K_f(\Theta)$, a state observer $\hat{P}(\Theta)$, observer gains $L(\Theta)$, a state feedback controller $K_S(\Theta)$, an integrator $I(q)$, and an integral error feedback controller $K_I(\Theta)$.

As shown in Fig. 2, the feedback controllers $K_S(\Theta)$ and $K_I(\Theta)$ and observer gains $L(\Theta)$ are designed for the the feed-forward controller $K_f(\Theta)$ compensated plant $P(\Theta)$. The feed-forward controller $K_f(\Theta)$ is designed using the inverse of $cG(q)$

$$K_f(\Theta) = \frac{G^{-1}(q)}{c} = \frac{1}{c}\left(\frac{1-(1-\alpha_k)q^{-1}}{\beta_k + (\alpha_k - \beta_k)q^{-1}}\right).$$

Also as depicted in Fig. 2, the LPV system $P(\Theta)$ is augmented with a state observer $\hat{P}(\Theta)$ to obtain the estimated states $\hat{x}_p$ of the plant. The observer $\hat{P}(\Theta)$ has the standard state space representation

$$\begin{aligned}\hat{x}_p(k+1) &= A_p(\Theta)\hat{x}_p(k) + B_w w_1(k) + B_p(\Theta)m_i(k) \\ &\quad + L(\Theta)(y_s(k) - \hat{y}_s(k)) \\ \hat{y}_s(k) &= C_p\hat{x}_p(k).\end{aligned} \tag{6}$$

Notice also in Fig. 2, the error between the output of the plant $y_s$ and the equivalence ratio set point $w_2$ is integrated by the numerical summation

$$I(q) = \frac{1}{q-1}$$

to obtain zero steady-state error.

To use $\mathcal{L}_2$ gain [20] for the performance criterion for shaping the frequency response of the closed-loop system, weighing functions (which can be considered as design parameters) are also introduced in Fig. 2. The weighting functions $W_1(q)$ and $W_2(q)$ are selected as follows:

$$\begin{aligned}W_1(q) &= \frac{0.1411}{q - 0.9986}, \\ W_2(q) &= \frac{0.0003982q + 0.0003979}{q^2 - 1.997178q + 0.997180},\end{aligned}$$

where $W_2$ was chosen as a second-order low-pass filter with a high DC gain to provide more weight on the low frequency signals since $w_2$ is the step input of the desired equivalence ratio.

From Fig. 2, the control input $u(k)$ and observer correction $u_L(k)$ are designed to be

$$\underbrace{\begin{bmatrix} u_{fb}(k) \\ u_L(k) \end{bmatrix}}_{u(k)} = \underbrace{\begin{bmatrix} K_S(\Theta) & K_I(\Theta) & 0 \\ 0 & 0 & L(\Theta) \end{bmatrix}}_{K(\Theta)} \underbrace{\begin{bmatrix} \hat{x}_p(k) \\ e_I(k) \\ e_y(k) \end{bmatrix}}_{e(k)} \tag{7}$$

where $\hat{x}_p \in \mathbb{R}^s$, $e_I \in \mathbb{R}$, $e_y \in \mathbb{R}$, $u_{fb} \in \mathbb{R}$, and $u_L \in \mathbb{R}^s$, such that the gain-scheduling controller that will be designed using [18] is $K(\Theta)$.

### B. Generalized Plant

With the variation of the wall-wetting parameters $\alpha$ and $\beta$ represented by $\alpha_\delta$ and $\beta_\delta$ and the engine speed, $v$, normalized to $\gamma$ as shown in [16], the generalized plant of all of the systems connected together inside the box of Fig. 2 is

written as a discrete-time LPV system with LFT parameter dependency,

$$\begin{bmatrix} l(k) \\ x(k+1) \\ z(k) \\ e(k) \end{bmatrix} = \underbrace{\left[\begin{array}{c|ccc} D_{00} & C_0 & D_{01} & D_{02} \\ \hline B_0 & A & B_1 & B_2 \\ 0 & C_1 & 0 & 0 \\ 0 & C_2 & 0 & 0 \end{array}\right]}_{=:M} \begin{bmatrix} p(k) \\ x(k) \\ \tilde{w}(k) \\ u(k) \end{bmatrix}, \quad (8)$$
$$p(k) = \Theta(k) l(k),$$

where $x(k) \in \mathbb{R}^n$ is the state at time $k$, $\tilde{w}(k) \in \mathbb{R}^r$ is the unweighted disturbance, $z(k) \in \mathbb{R}^p$ is the error output, $p(k), l(k) \in \mathbb{R}^{n_p}$ are the pseudo-input and output connected by $\Theta(k)$, $u(k) \in \mathbb{R}^m$ is the control input, and $e \in \mathbb{R}^m$ is the measurement for control. The generalized plant $H(\Theta)$ is displayed in the standard LFT configuration on the right hand side of Fig. 3. As depicted in Fig. 3, the generalized plant $H(\Theta)$ is represented by the LFT interconnections inside the dashed box. The time-varying parameter $\Theta$ in Eq. (8) follows the structure

$$\begin{aligned} \Theta \in \mathbf{\Theta} = &\{\text{diag}(\beta_\delta I_4, \alpha_\delta I_3, \gamma I_{18}) : \\ &|\alpha_\delta| \le \delta_1, |\beta_\delta| \le \delta_2, |\gamma| \le 1\}, \end{aligned} \quad (9)$$

where $\delta_1 = \frac{\overline{\alpha}-\underline{\alpha}}{2}$ and $\delta_2 = \frac{\overline{\beta}-\underline{\beta}}{2}$.

The $\ell_2$ gain of the LPV system in Eq. (8) with a gain-scheduling feedback controller is defined as

$$\max_{\Theta \in \mathbf{\Theta}, \|w\|_2 \neq 0} \frac{\|z\|_{\ell_2}}{\|\tilde{w}\|_{\ell_2}}. \quad (10)$$

Now we formally state the gain-scheduling control design problem.

**Problem :** The goal is to design a static gain-scheduling control $u(k) = K(\Theta)e(k)$ that stabilizes the closed-loop system and minimizes the worst-case $\ell_2$ gain ($\mathcal{H}_\infty$ norm) of the closed-loop LPV system in Eq. (8) for any trajectories of $\Theta(k) \in \mathbf{\Theta}$.

The gain-scheduling method provided by [18] can be applied for discrete-time polytopic time-varying systems. A polytopic system requires that the system matrices for any set of time-varying parameters can be represented as a convex combination of the vertex system matrices of the parameter space polytope. This implies that the parameter variation must be affine. However, since $D_{00}$ of the LPV system in in Eq. (8) is a non-zero matrix, the system matrices are not affine functions of the time-varying parameters. Therefore, in the next section, we will compute the first-order Taylor series expansion of the generalized plant to obtain systems matrices with affine parameter variation.

### *C. First-order Taylor Series Expansion of the Generalized Plant*

To utilize the control synthesis technique in [18], we calculate the first-order Taylor series approximation of the system matrices to obtain affine functions in $\Theta$. Notice that Eq. (8) is an upper LFT, i.e.,

$$H(\Theta) := \mathcal{F}_u(M, \Theta). \quad (11)$$

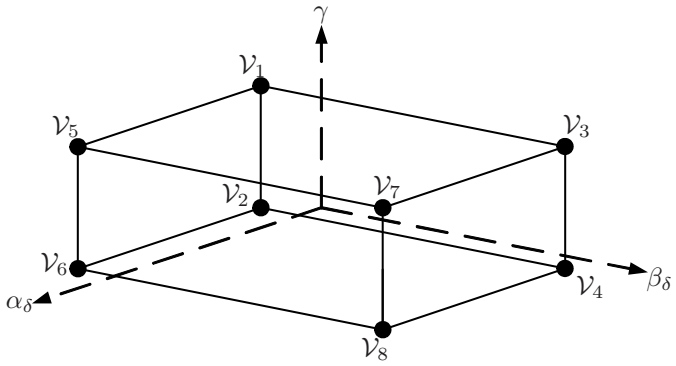


Fig. 4. Parameter space polytope.

Using the Taylor series expansion at $\Theta = 0$, the system can be approximated as

$$\hat{H}(\Theta) = H(0) + \beta_\delta \left[\nabla H(0)\right]_1 + \alpha_\delta \left[\nabla H(0)\right]_2 + \gamma \left[\nabla H(0)\right]_3, \quad (12)$$

where $\left[\nabla H(0)\right]_i$ is the partial derivative of the LFT system $H(\Theta)$ in Eq. (11) with respect to the $i$-th parameter, which can be calculated as shown in [21]. The approximation of the generalized plant $H(\Theta)$ to $\hat{H}(\Theta)$ is depicted in Fig. 3. Using the affine system matrices $\hat{H}(\Theta)$, the polytopic system can be computed and the controller synthesis, which is covered in the next section, can be performed.

### *D. Control Synthesis for polytopic linear time-varying system*

The gain-scheduling method provided by [18] is designed for discrete-time polytopic time-varying systems. The affine system matrices $\hat{H}(\Theta)$ in Eq. (12) can be converted into the discrete-time polytopic time-varying system (Eq. (13)) by solving for the state-space matrices at vertices $\{\mathcal{V}_i\}$ of the parameter space polytope displayed in Fig. 4. Any system inside of the convex parameter set is represented by a convex combination of the vertex systems. The discrete-time polytopic linear time-varying system is given by

$$\begin{bmatrix} x(k+1) \\ z(k) \\ e(k) \end{bmatrix} = \begin{bmatrix} \bar{A}[\lambda(k)] & \bar{B}_1[\lambda(k)] & \bar{B}_2[\lambda(k)] \\ \bar{C}_1[\lambda(k)] & \bar{D}_{11}[\lambda(k)] & \bar{D}_{12}[\lambda(k)] \\ \bar{C}_2 & 0 & 0 \end{bmatrix} \begin{bmatrix} x(k) \\ w(k) \\ u(k) \end{bmatrix}, \quad (13)$$

where, for all $k \in \mathbb{Z}_{\ge 0}$, $\lambda(k)$ is the vector of time-varying barycentric coordinates that belong to the unit simplex

$$\Lambda_N = \left\{ \zeta \in \mathbb{R}^N : \sum_{i=1}^{N} \zeta_i = 1, \zeta_i \ge 0, i = 1, \cdots, N \right\}.$$

A way to compute the barycentric coordinate vector $\lambda(k)$ for a given $\alpha_\delta(k)$, $\beta_\delta(k)$, and $\gamma(k)$ is provided by [22]. For all $k \in \mathbb{Z}_{\ge 0}$, the rate of variation of the weights

$$\Delta\lambda_i(k) = \lambda_i(k+1) - \lambda_i(k), \quad i = 1, \cdots, N$$

is limited by the calculated bound $b$ such that

$$-b\lambda_i(k) \le \Delta\lambda_i(k) \le b(1 - \lambda_i(k)), \quad i = 1, \cdots, N \quad (14)$$

where $b \in [0, 1]$.

The system matrices $\bar{A}[\lambda(k)] \in \mathbb{R}^{n\times n}$, $\bar{B}_1[\lambda(k)] \in \mathbb{R}^{n\times r}$, $\bar{B}_2[\lambda(k)] \in \mathbb{R}^{n\times m}$, $\bar{C}_1[\lambda(k)] \in \mathbb{R}^{p\times n}$, $\bar{D}_{11}[\lambda(k)] \in \mathbb{R}^{p\times r}$, $\bar{D}_{12}[\lambda(k)] \in \mathbb{R}^{p\times m}$ belong to the polytope

$$\mathcal{D} = \{(\bar{A}, \bar{B}_1, \bar{B}_2, \bar{C}_1, \bar{D}_{11}, \bar{D}_{12})(\lambda(k)) : (\bar{A}, \bar{B}_1, \bar{B}_2, \bar{C}_1, \bar{D}_{11}, \bar{D}_{12})(\lambda(k)) = \sum_{i=1}^{N} \lambda_i(k)(\bar{A}, \bar{B}_1, \bar{B}_2, \bar{C}_1, \bar{D}_{11}, \bar{D}_{12})_i, \lambda(k) \in \Lambda_N\}.$$

A finite set of LMIs in [18] can be used to design the gain-scheduling controller $K(\Theta)$ in Eq. (7). Due to Theorem 3 of [18], if there exists matrices $G_{i,2} \in \mathbb{R}^{(n-q)\times q}$, $G_{i,3} \in \mathbb{R}^{(n-q)\times(n-q)}$, $G_{i,fb} \in \mathbb{R}^{(s+1)\times(s+1)}$, $G_{i,L} \in \mathbb{R}$, $Z_{i,fb} \in \mathbb{R}^{1\times(s+1)}$, and $Z_{i,L} \in \mathbb{R}^{s\times 1}$ such that

$$G_{i,1} = \begin{bmatrix} G_{i,fb} & 0 \\ 0 & G_{i,L} \end{bmatrix}, \quad \text{and} \quad Z_{i,1} = \begin{bmatrix} Z_{i,fb} & 0 \\ 0 & Z_{i,L} \end{bmatrix}$$

and symmetric matrices $P_i \in \mathbb{R}^{n\times n}$ such that the LMI conditions in [18] are satisfied, the gain-scheduling static feedback control is then obtained as

$$K(\lambda(k)) = \hat{Z}(\lambda(k))\hat{G}(\lambda(k))^{-1}, \tag{15}$$

where

$$\hat{Z}(\lambda(k)) = \sum_{i=1}^{N} \lambda_i(k) Z_{i,1} \quad \text{and} \quad \hat{G}(\lambda(k)) = \sum_{i=1}^{N} \lambda_i(k) G_{i,1}.$$

This control is proved to stabilize affine parameter-dependent systems such as (13) with a guaranteed $\mathcal{H}_\infty$ performance bounded by $\eta$ for all $\lambda \in \Lambda_N$ and $\Delta\lambda$ that satisfies (14).

## IV. Simulation Results

The performance of the dynamic gain-scheduling controller developed in this paper is demonstrated by comparing its measured equivalence ratio response to the response of the gain-scheduling PID controller developed in [17]. To ensure that the comparison is fair, the weighting functions $W_1(q)$ and $W_2(q)$ used to design the dynamic gain-scheduling controller are the exact same as those used to design the gain-scheduling PID controller in [17]. Each gain-scheduling controller is simulated with the a crank resolved mean-value engine model developed in [23].

### A. Step Throttle Change

In this case we simulate an engine dynamometer experiment for an engine operated at a temperature of $120°C$ with an engine speed of $1500$ rpm. After the engine is stably operated at this condition with a $32\%$ throttle, the load is increased by a step throttle position from $32\%$ to $46\%$. Note that in the dynamometer test, the engine speed was maintained by the dynamometer through torque regulation. This is similar to the driving condition that a step throttle is applied to maintain the vehicle speed when the vehicle is driven up a hill. Note that the step increment of throttle position produces a slight change in the wall-wetting parameter $\beta$ as shown in Fig. 5C. The measured equivalence ratio of the engine model with each controller is given in Fig. 5A. The throttle step occurring at the $30^{th}$ second results in a drop in the equivalence ratio due to the step air mass flow. In the detail of Fig. 5A, we see that while the measured equivalence ratio with both gain-scheduling controllers drops to just under $0.85$, the gain- scheduling PID controller proceeds to overshoot $1.00$ by about $0.01$ while the dynamic gain- scheduling controller never exceeds $1.00$. We also note that the dynamic gain-scheduling controller uses less fuel than the gain-scheduling PID controller as shown in Fig. 5B.

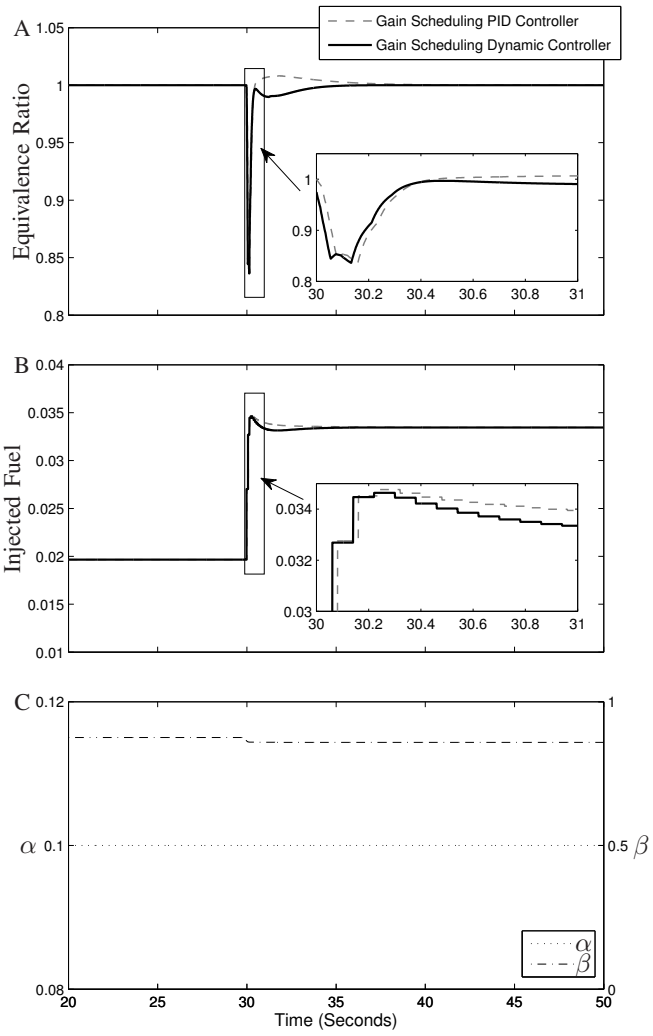


Fig. 5. Step Throttle Change Simulation

### B. Engine Speed Change

In this simulation, an engine was operated on a dynamometer with its coolant temperature at $120°C$. To demonstrate the capability for the gain scheduling controller to handle engine speed variations, a smoothed step command from $1500$ rpm to $2500$ rpm was applied to the engine dynamometer to manipulate the engine speed as shown in Fig. 6D. The resulting engine wall-wetting dynamics parameters, shown in Fig. 6C, were used in the simulation. Notice in Fig. 6A that while the gain-scheduling PID con-

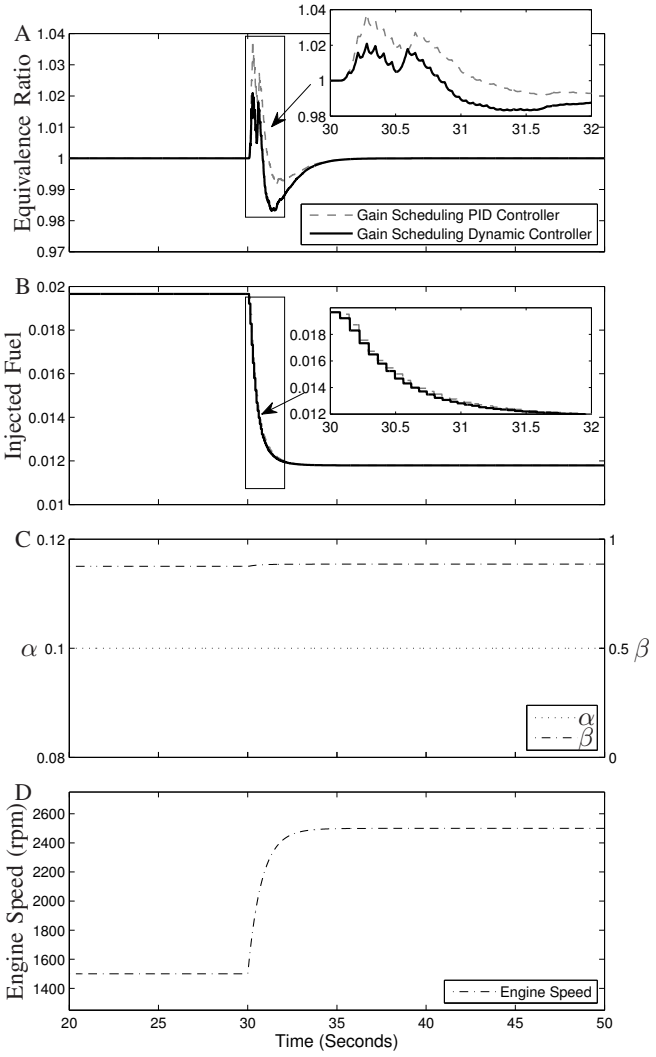


Fig. 6. Engine Speed Change Simulation

troller regulates the measured equivalence ratio within $4\%$ of the target value, the dynamic gain-scheduling controller outperforms it by regulating the measured equivalence ratio within $2\%$ of the target value of $1.00$. We also note that while there is not too much difference in fueling as shown in Fig 6B, in the detail we can see that the dynamic gain-scheduling controller uses slightly less fuel than the gain-scheduling PID controller.

## V. Conclusion

In this paper, an event-based dynamic gain-scheduling controller was designed by employing a standard control structure of observer-based state feedback with integral control. The dynamic gain-scheduling controller was applied to an LPV system representing the air-to-fuel ratio control of a port-fuel-injection process. The system parameters used in the engine fuel system model are engine speed, temperature, and load. The static gains of the dynamic gain-scheduling controller for the obtained LPV system were then designed based on the numerically efficient convex optimization (or LMI) technique. The simulation results demonstrate the effectiveness of the proposed scheme.

## References


[1] J. Rivard, "Closed-Loop Electronic Fuel Injection Control of the Internal-Combustion Engine," *SAE 730005*, 1973.

[2] J. Cassidy Jr and M. Athans, "On the design of electronic automotive engine controls using linear quadratic control theory," *IEEE Transactions on Automatic Control*, vol. 25, no. 5, pp. 901–912, 1980.

[3] W. Powers, B. Powell, and G. Lawson, "Applications of optimal control and Kalman filtering to automotive systems," *International Journal of Vehicle Design Special Publication SP4*, 1983.

[4] N. Benninger and G. Plapp, "Requirements and performance of engine management systems under transient conditions," *SAE 910083*, 1991.

[5] C. Onder, "Model-Based Multivariable Speed and Air-To-Fuel Ratio Control of An SI Engine," *SAE 930859*, 1993.

[6] S. Choi, J. Hedrick, V. Kelsey-Hayes, and M. Livonia, "An observer-based controller design method for improving air/fuel characteristics of spark ignition engines," *IEEE Transactions on Control Systems Technology*, vol. 6, no. 3, pp. 325–334, 1998.

[7] R. C. Turin and H. P. Geering, "Model-Reference Adaptive A/F Ratio Control in an SI Engine Based on Kalman-Filtering Techniques," *Proceedings of American Control Conference*, pp. 4082–4090, 1996.

[8] Y. Yildiz, A. Annaswamy, D. Yanakiev, and I. Kolmanovsky, "Adaptive Air Fuel Ratio Control for Internal Combustion Engines," *Proceedings of American Control Conference*, pp. 2058–2063, 2008.

[9] J. Powell, N. Fekete, and C. Chang, "Observer-Based Air-Fuel Ratio Control," *IEEE Control Systems Magazine*, vol. 18, pp. 72–83, 1998.

[10] L. Mianzo, H. Peng, and I. Haskara, "Transient Air-Fuel Ratio $H_\infty$ Preview Control of a Drive-By-Wire Internal Combustion Engine," *Proceedings of American Control Conference*, pp. 2867–2871, 2001.

[11] K. R. Muske and J. C. P. Jones, "A Model-based SI Engine Air Fuel Ratio Controller," *Proceedings of American Control Conference*, pp. 3284–3289, 2006.

[12] S. Pace and G. G. Zhu, "Sliding Mode Control of a Dual-Fuel System Internal Combustion Engine," in *Proceedings of ASME Dynamic Systems and Control Conference*, Hollywood, CA, October 2009.

[13] A. U. Genç, "Linear Parameter-Varying Modelling and Robust Control of Variable Cam Timing Engines," Ph.D. dissertation, University of Cambridge, 2002.

[14] F. Zhang, K. M. Grigoriadis, M. A. Franchek, and I. H. Makki, "Linear Parameter-Varying Lean Burn Air-Fuel Ratio Control for a Spark Ignition Engine," *Journal of Dynamic Systems, Measurement and Control*, vol. 192, pp. 404–414, 2007.

[15] R. A. Zope, J. Mohammadpour, K. M. Grigoriadis, and M. Franchek, "Air-fuel ratio control of spark ignition engines with TWC using LPV techniques," *Proceedings of ASME Dynamic Systems and Control Conference*, 2009.

[16] A. White, J. Choi, R. Nagamune, and G. Zhu, "Gain-scheduling control of port-fuel-injection processes," *IFAC Journal of Control Engineering Practice*, 2011, DOI: 10.1016/j.conengprac.2010.12.007.

[17] A. White, G. Zhu, and J. Choi, "Hardware-in-the-Loop Simulation of Robust Gain-Scheduling Control of Port-Fuel-Injection Processes," *IEEE Transaction on Control System Technology*, 2011, DOI: 10.1109/TCST.2010.2095420.

[18] J. Caigny, J. Camino, R. Oliveira, P. Peres, and J. Swevers, "Gain scheduled $H_\infty$-control of discrete-time polytopic time-varying systems," in *Proceedings of Conference on Decision and Control*, 2008, pp. 3872–3877.

[19] A. Balluchi, L. Benvenuti, M. D. di Benedetto, C. Pinello, A. L. Sangiovanni-Vincentelli, and R. PARADES, "Automotive engine control and hybrid systems: challenges and opportunities," *Proceedings of the IEEE*, vol. 88, no. 7, pp. 888–912, 2000.

[20] H. K. Khalil, *Nonlinear Systems*. Prentice Hall, 2002.

[21] R. Nagamune and J. Choi, "Parameter reduction of estimated model sets for robust control," *Journal of Dynamic Systems, Measurement, and Control*, vol. 132, no. 2, March 2010, DOI: 10.1115/1.4000661.

[22] J. Warren, S. Schaefer, A. N. Hirani, and M. Desbrun, "Barycentric coordinates for convex sets," *Advances in Computational Mathematics*, vol. 27, no. 3, pp. 319–338, 2007.

[23] X. Yang and G. G. Zhu, "A Mixed Mean-Value and Crank-Based Model of a Dual-Stage Turbocharged SI Engine for Hardware-In-the-Loop Simulation," in *Proceedings of 2010 American Control Conference*, Baltimore, MD, June 2010.